Published online 23 November 2021 *Nucleic Acids Research, 2021, Vol. 49, No. 21* **12035–12047**
https://doi.org/10.1093/nar/gkab922

Cisplatin fastens chromatin irreversibly even at a high chloride concentration

Hyeon-Min Moon[1,2,†], Jin-Sung Park[1,†], Il-Buem Lee[1,2], Young-Im Kang[2], Hae Jun Jung[2], Dongju An[3], Yumi Shin[3], Min Ji Kim[4], Hugh I. Kim[4], Ji-Joon Song[3], Jaehoon Kim[3], Nam-Kyung Lee[5] and Seok-Cheol Hong[1,2,*]

[1]Center for Molecular Spectroscopy and Dynamics, Institute for Basic Science, Seoul 02841, Korea, [2]Department of Physics, Korea University, Seoul 02841, Korea, [3]Department of Biological Sciences, Korea Advanced Institute of Science and Technology, Daejeon 34141, Korea, [4]Department of Chemistry, Korea University, Seoul 02841, Korea and [5]Department of Physics, Sejong University, Seoul 05006, Korea

Received February 27, 2021; Revised September 12, 2021; Editorial Decision September 26, 2021; Accepted September 28, 2021

ABSTRACT

Cisplatin is one of the most potent anti-cancer drugs developed so far. Recent studies highlighted several intriguing roles of histones in cisplatin's anti-cancer effect. Thus, the effect of nucleosome formation should be considered to give a better account of the anti-cancer effect of cisplatin. Here we investigated this important issue via single-molecule measurements. Surprisingly, the reduced activity of cisplatin under [NaCl] = 180 mM, corresponding to the total concentration of cellular ionic species, is still sufficient to impair the integrity of a nucleosome by retaining its condensed structure firmly, even against severe mechanical and chemical disturbances. Our finding suggests that such cisplatin-induced fastening of chromatin can inhibit nucleosome remodelling required for normal biological functions. The *in vitro* chromatin transcription assay indeed revealed that the transcription activity was effectively suppressed in the presence of cisplatin. Our direct physical measurements on cisplatin-nucleosome adducts suggest that the formation of such adducts be the key to the anti-cancer effect by cisplatin.

GRAPHICAL ABSTRACT

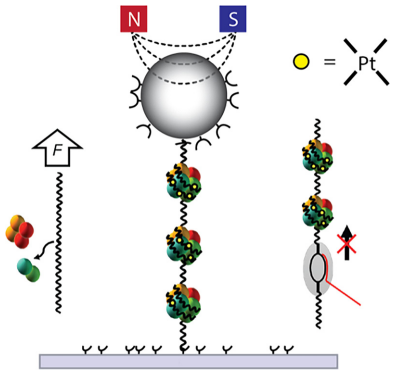

INTRODUCTION

Cisplatin, *cis*-[$PtCl_2(NH_3)_2$], is a platinum-based chemotherapy agent widely used to treat a variety of human cancers (1,2). Its primary target is DNA and formation of cisplatin-DNA adducts is required for its pharmacological effect. It binds preferentially to the N7 nitrogen atoms of two purine bases and causes local DNA kinks, subsequently triggering DNA repair, apoptosis, or necrosis (3–7). Thus, understanding the physical characteristics of cisplatin-DNA adducts is a critical issue for elucidating and improving the anti-cancer effect of cisplatin and for subduing its severe cytotoxicity and avoiding cisplatin resistance so as to broaden its application.

The mechanism for efficient delivery of cisplatin into a cell and its action on nuclear DNA have been extensively studied over decades and significant progress has been made based on chemical, biochemical and structural biology analyses. In the Cl^--rich extracellular space (∼140 mM), cisplatin exists in the neutral, dichloro form, *cis*-[$PtCl_2(NH_3)_2$], which is not reactive with most nu-

*To whom correspondence should be addressed. Tel: +82 2 3290 3112; Email: hongsc@korea.ac.kr
†These authors wish it to be known that, in their opinion, the first two authors should be regarded as joint First Authors.

cleophiles and diffuses across a cellular lipid bilayer. Since the intracellular concentration of Cl^- is very low (~10 mM), cisplatin becomes hydrolysed into monovalent (*cis*-$[PtCl(H_2O)(NH_3)_2]^+$) or divalent cations (*cis*-$[Pt(H_2O)_2(NH_3)_2]^{2+}$) by releasing Cl^- upon cell entry. These cationic forms of cisplatin, which accumulate inside a cell, are the active agents that bind to most nucleophiles including N^7 nitrogen in guanine. In other words, the formation of charged, hydrolysed cisplatin due to low intracellular [Cl^-] is an essential element of this model. However, other anionic species such as acetates, carbonates, phosphates, and thiolates that are common inside cells are also known to interfere with cisplatin binding by effectively competing with DNA (8,9).

Another important factor that deserves due attention is the complexity originating from packaging of DNA into chromatin, form that cellular DNA adopts. Recent studies emphasized multi-faceted involvements of chromatin in various events triggered by cisplatin. It has been demonstrated that cisplatin hampers transcription by interfering with opening of chromatin structures and by blocking transcription factor binding directly (10), inhibition of histone deacetylase increases cytotoxicity by cisplatin (11), nucleosome assembly significantly inhibits nucleotide excision repair, primary repair pathway for damage caused by cisplatin (7), cisplatin treatment causes post-translational modifications of histones H3 and H4, which may induce structural alterations and rearrangements of chromosomes (12), 1,2-dGpG cisplatin crosslink influences the translational and rotational setting of DNA in nucleosomes (13), the nucleosomal packaging of DNA modulates the overall pattern of cisplatin binding to DNA and facilitates site-selective transfer of cisplatin to nearby dGpG sites via the central part of core histones (14), and the formation of platinum drug adducts in the nucleosome core reduces nucleosome mobility (15).

In this report, we investigated the effect of cisplatin on a nucleosomal DNA (N-DNA) molecule in 180 mM NaCl solution. We directly showed that histones are irreversibly trapped upon cisplatin binding using magnetic tweezers (MT). Although the binding efficiency of cisplatin at such a high NaCl concentration is significantly reduced, the fastening of N-DNA by cisplatin appeared efficient enough to fix its structure against severe mechanical and ionic disturbances. The *in vitro* transcription assay with cisplatin-bound chromatin revealed that the transcription of a gene within the chromatin was effectively interfered by application of cisplatin. Our biophysical results are straightforward and direct in verifying the mechanistic role of histones implicated in cisplatin's anti-cancer activity.

MATERIALS AND METHODS

Sample preparation

Cisplatin and salts used in this study were all purchased from Sigma-Aldrich. Before reacting with DNA samples, cisplatin was fully dissolved for >1 day in reaction buffer at 37°C. Recombinant histone H2A/H2B dimers and H3.1/H4 tetramers were purchased from NEB (New England Biolabs, USA). The DNA tethers used in our single-molecule studies were prepared as previously (16), except for attachment chemistry, that is, copper-free click chemistry to covalently attach a single DNA molecule to the flow chamber surface (17). A 15-kb DNA plasmid was digested by BamHI and SacI (NEB, USA) and its longer fragment (~12 kb) was used as a main body of DNA tether. Biotinylated short DNA fragments (linkers) were prepared by PCR using biotin-dUTP (Roche, Switzerland) and subsequent digestion by SacI. For di-benzyl-cyclooctyne (DBCO) linkers, 5-DBCO-PEG_4-dUTP (Sigma-Aldrich, USA) was used instead in PCR and BamHI was used to digest them. The linearized plasmid DNA was then ligated to a biotin linker at one end for specific attachment to a streptavidin-coated magnetic bead and a DBCO linker at the other end also for specific attachment to the azide-coated glass substrate of the sample chamber via copper-free click chemistry.

NAP1 purification

Mouse NAP1 (nucleosome assembly protein 1) in a modified pET28a vector was expressed with an N-terminal His-tag from BL21(DE3) *Escherichia coli*. The cells were lysed with sonication in a buffer containing 50 mM Tris–HCl (pH 8.0), 100 mM NaCl and 5% glycerol (Buffer A). The cell debris were cleared by centrifugation at 12,000 rpm for 30 min. The supernatant was incubated with Ni-NTA beads. The beads were collected and washed with a buffer A containing 20 mM imidazole. The proteins were eluted with a buffer A containing 100 mM imidazole. The proteins were further purified with HiTrap Q anion exchange chromatography followed by Superdex S200 gel filtration chromatography equilibrated with 20 mM HEPES (pH 7.5) and 100 mM KCl.

Nucleosome assembly assay

Nucleosome assembly is achieved enzymatically *in vivo* by histone chaperones together with other assembly factors. Similarly, we assembled N-DNA with NAP1 successfully under a mild ionic condition (18,19). The high integrity of NAP1-induced N-DNA was demonstrated by regular band pattern in the standard micrococcal nuclease (MNase) digestion assay (Supplementary Figure S1). To prepare nucleosomes for single-molecule MT assays, a mixture of core histones (H3.1/H4: 150 nM, H2A/H2B: 400 nM) and 500 nM NAP1 was incubated in the buffer with 50 mM KCl, 25 mM HEPES at pH 7.6, 0.1 mM EDTA, 0.25% PEG, 0.25% polyvinyl alcohol (PVOH) and 1 mg/ml BSA on ice for 30 min. To ensure complete nucleosome assembly, we used higher molar concentrations of H2A/H2B than those of H3.1/H4 (20,21). Before the NAP1-histone mixture was released into the flow chamber for nucleosome assembly on the surface-bound DNA tether, the mixture was diluted by 100–1000-fold in the reaction buffer composed of 25 mM HEPES at pH 7.6, 50 mM KCl, 0.1 mM EDTA, 0.025% (v/v) PEG and 0.025% (v/v) PVOH.

In vitro transcription assay

Procedures for recombinant chromatin assembly and standard activator- and coactivator-dependent *in vitro* tran-

scription assay were described elsewhere (22). For chromatin assembly, core histone octamer (350 ng) and NAP1 (2.5 μg) in 55 μl HEG buffer (25 mM HEPES (pH 7.6), 0.1 mM EDTA, and 10% glycerol) was incubated on ice for 30 min. After addition of ACF complex (70 ng) and p53ML plasmid (350 ng), the reaction was adjusted to 25 mM HEPES (pH 7.6), 50 mM KCl, 5 mM $MgCl_2$, 0.1 mM EDTA, 10% glycerol and 3.2 mM ATP in a final volume of 70 μl and incubated at 27°C for 4 h. The p53ML plasmid contains five p53 binding sites and the adenovirus major late promoter followed by a G-less cassette that produces 390-nucleotide transcripts.

The *in vitro* transcription assay from chromatin template was performed as outlined in Figure 5D. Specifically, (i) the assembled chromatin (8 μl, 40 ng DNA) was incubated with cisplatin (0, 0.17 or 0.33 mM in a 15 μl reaction mixture with [Cl^-] ∼120 mM, further diluted to 0, 0.05 or 0.1 mM in a final volume of 50 μl transcription reaction) at 27°C for 15 min in a 15 μl reaction; (ii) the cisplatin-treated chromatin was incubated with p53 (20 ng) in 0.5× HAT buffer (10 mM HEPES (pH 7.8), 30 mM KCl, 2.5 mM DTT, 0.25 mM EDTA and 5 mM sodium butyrate) at 30°C for 20 min in a 20 μl reaction; (iii) the p53-bound chromatin was incubated with p300 (10 ng) and 20 μM acetyl coenzyme A at 30°C for 30 min in a 25 μl reaction; (iv) pre-initiation complex was formed at 30°C for 20 min by addition of 5 μl HeLa nuclear extracts (10 mg/ml), 1 μl DTT (250 mM), and 2.5 μl 20× RB buffer (400 mM HEPES (pH 7.8), 120 mM $MgCl_2$) and BC200 buffer (20 mM Tris HCl (pH 7.9), 200 mM KCl, 0.2 mM EDTA and 20% glycerol) was added, along with water to adjust the final KCl concentration to 65 mM in a 45.5 μl reaction; (v) 2.5 μl 20× nucleotide mixture (10 mM ATP, 10 mM CTP, 0.5 mM UTP and 2 mM 3′-*O*-methyl-GTP), 1 μl [α-^{32}P] UTP (10 μCi/μl, 3000 Ci/mmol) and 1 μl RNasin (10 U/μl) were added to adjust the final volume to 50 μl, and transcription was allowed to proceed for 50 min at 30°C; (vi) the reaction was stopped with addition of 150 μl stop buffer (150 mM sodium acetate (pH 5.2), 0.5% SDS, and 10 mM EDTA) and further incubated at 37°C for 30 min with inclusion of 30 μg proteinase K; (vii) radiolabelled RNA was extracted with phenol/chloroform/isoamyl alcohol (25:24:1), precipitated by ethanol, resolved on 5% polyacrylamide gel (19:1) containing 8 M urea and analysed by autoradiography.

Magnetic tweezers assay

The detailed description for our MT setup was given elsewhere (16), so the essential information will be summarized here (see Supplementary Figure S2). Magnetic-bead-bound DNA tethers were pulled by a pair of magnets. In our setup, the magnets can exert a force up to ∼6 pN to a 1 μm-sized magnetic bead and a force up to ∼100 pN to a 2.8 μm-sized magnetic bead. To measure the force to the beads, we utilized Brownian fluctuations of the beads monitored at 60 Hz in real time by a CMOS camera (MV1-D1024E-160-Cl-12, Photonfocus). The force exerted on a DNA molecule was basically calculated by the usual equipartition theorem, $F = k_B\,Tl/\langle\Delta x^2\rangle$, where k_BT is the thermal energy, l the extension of DNA tether, and $<\Delta x^2>$ the lateral fluctuations of the bead and was corrected by a spectral analysis method (23). The vertical position of the bead necessary to determine l was obtained by analysing the diffraction ring pattern of the bead. To fit the force-extension data of DNA, we used the worm-like chain (WLC) model given by $\frac{F\xi_p}{k_BT} = \frac{l}{L} + \frac{1}{4(1-l/L)^2} - \frac{1}{4}$, where L is the contour length of DNA (24).

For our MT assays, we used torsionally-free DNA (i.e. nicked DNA) to avoid any unnecessary complications caused by DNA supercoiling during the assembly of nucleosomes. After injecting NAP1 and histones into the chamber, free NAP1 and histones were washed out in 30 min by exchanging buffers. Then, N-DNA molecules were treated with cisplatin for 1 hour. After washing free cisplatin out with PBS, we measured the mechanical behaviour of cisplatin-bound N-DNA. One parameter to consider here is a stoichiometric parameter, r value, defined by the ratio of drug concentration to basepair (bp) concentration, [drug]/[DNA bp]. It would be a useful rule of thumb to compare the stoichiometry of bulk assays with that of single-molecule assays. In our *in vitro* gel assays, the r values in 3.3- and 0.1-mM cisplatin solutions are 871 and 26, respectively. Assuming a single DNA molecule occupies a space of 1 × 1 × 5 μm^3, the amount of cisplatin contained in this volume would be 1.65×10^{-17} and 5×10^{-19} moles for 3.3- and 0.1-mM cisplatin solutions, respectively. Thus, the r values are 824 and 25 for 3.3- and 0.1-mM cisplatin solutions, respectively. Interestingly, these r values from our bulk and single-molecule assays are very close to each other.

RESULTS

Salt-sensitive binding efficiency of cisplatin to DNA estimated from biophysical measurements

It has been of great interest to directly measure altered mechanical properties of DNA due to crosslinking by intercalating agents at the single-molecule level (25–29). We have developed a method to estimate the binding efficiency of cisplatin to DNA via single molecule force-extension measurements of DNA and the bimodal modelling that relates the degree of cisplatin binding to the elasticities of a cisplatin-bound DNA tether in the low- and high-tension regimes (25,26). Our bimodal analysis has several advantages: although the WLC model with a single persistence length (ξ_p) gives a reasonable fit as demonstrated in other reports (30,31), our bimodal analysis captures the microscopic picture of cisplatin binding to DNA and enables us to determine the degree of cisplatin binding in a self-consistent manner. We also observed that high chloride concentration suppresses cisplatin binding to DNA. Here, we present our data that demonstrate this via single-molecule MT measurements under various salt conditions. At 3.3 mM cisplatin and 180 mM NaCl, no change in the persistence length of DNA (ξ_p) was observed (data not shown). At lower salt concentrations, ξ_p departs appreciably from the well-known value of ξ_p as shown in Figure 1 and Supplementary Table S1. According to Lee *et al.* (25,26), the fractions of cisplatin-bound base pairs (p) for [NaCl] = 90, 60 and 20 mM are 0.005 ± 0.001, 0.024 ± 0.003, and 0.069 ± 0.002, respectively. It is of note that the ξ_p of bare DNA is nearly constant around 50 nm in the broad range

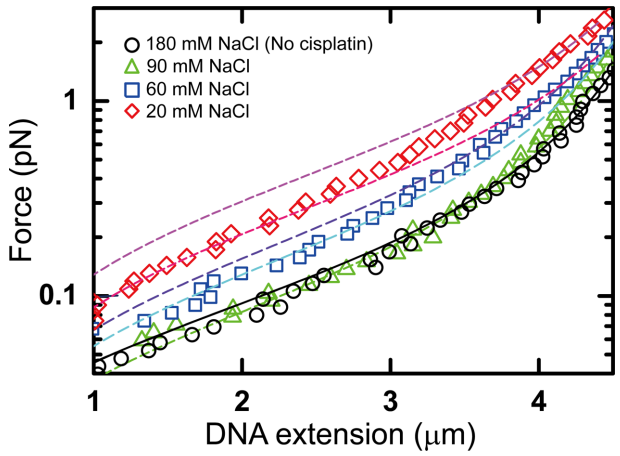

Figure 1. Force-extension curves of DNA incubated with 3.3 mM cisplatin in buffers with different NaCl concentrations. The dotted lines are fits by the WLC model. For [NaCl] = 20 and 60 mM, the high- and low-tension regimes are fitted separately (pink and red for [NaCl] = 20 mM, and blue and cyan for [NaCl] = 60 mM with the first (second) of each pair covering the high- (low-) tension regime) as described by the bimodal modeling (25,26) while the entire range for [NaCl] = 90 mM can be nicely fitted with a single persistence length (green). For comparison, the force-extension curve of bare DNA (black circle) measured in [NaCl] = 180 mM was overlaid with a WLC model fit (black).

of [NaCl] = 20∼180 mM. Recent single-molecule measurements have provided direct evidence for the near constancy (∼50 nm) of ξ_p in the range of mild salt concentrations ([NaCl] = 20–250 mM) (32–34). We would also point out that DNA tends to be slightly stiffer at low salt concentration by electrostatic repulsion, that is, reduced salt concentration by itself would increase ξ_p slightly, which is opposite to the decrease of ξ_p observed in our work by increased cisplatin binding to DNA at low salt concentration. Thus, we can safely rule out that the reduction of ξ_p observed in our assay at low salt condition is of electrostatic origin.

To cross-check the salt-dependent binding efficiency of cisplatin to DNA, we quantified the amount of cisplatin-DNA adducts using the Inductively Coupled Plasma-Mass Spectrometry (ICP-MS) (Supplementary Table S2 and see Supplementary materials and methods). When DNA was incubated with 3.3 mM cisplatin in a low salt concentration ([NaCl] ≤ 60 mM), the DNA sample could not be successfully purified for the ICP-MS assay as strongly crosslinked DNA molecules could not be recovered from filtration. Thus, for 3.3 mM cisplatin, we only performed the ICP-MS quantification of DNA and Pt at [NaCl] = 90 and 180 mM. As shown in the MT assay (Figure 1), the binding efficiency of cisplatin measured in the ICP-MS assay was higher for lower [NaCl] (with [NaCl] = 180 → 90 mM, $P = 0.07 \rightarrow 0.12$). In [cisplatin] = 0.1 mM, we were able to acquire the ICP-MS quantification of DNA and Pt over the whole range of [NaCl] (0–180 mM) as massively crosslinked DNA was avoided. As expected, the binding affinity of cisplatin decreased with [NaCl]. p is however consistently higher in the ICP-MS assay than in the MT assay likely due to the existence of mono-functional cisplatin (8,35). The ICP-MS assay measures both mono- and bi-functional adducts while only the latter contributes to the elastic property of DNA. Another possible source for discrepancy is incomplete removal of unbound cisplatin before ICP-MS measurements. In any event, the correlation between p and [NaCl] is clear.

Cisplatin can induce more dramatic collapse of bare DNA under weak tension (Supplementary Figure S3). After a 30-min incubation with 3.3 mM cisplatin in a buffer with [NaCl] = 10 mM, the magnetic force (F) was reduced to 0.4 pN without washing free cisplatin out. Then, cisplatin-bound DNA was suddenly condensed, which is reminiscent of DNA condensations mediated by looping proteins (36,37). This sudden condensation of DNA occurred in steps. The irreversible DNA condensation by cisplatin suggests that free cisplatin pinches a transient DNA loop and crosslinks two (distal) segments of the same DNA strand (in the intermediate salt conditions, a transient cisplatin monofunctional adduct may capture a distal DNA segment and form a DNA loop when the segment collides with it) as reported previously (28) and the size of a step is in the range of 25–500 nm (Supplementary Figure S3B and C). In a buffer with [NaCl] > 30 mM, such a drastic condensation of DNA did not happen (data not shown). This shows that cisplatin can join distal segments of the same DNA molecule, suggesting that such a binding mode play a role in trapping nucleosome particles as proposed below.

The effects of numerous ion species on DNA platination have been previously investigated as cisplatin acts in the presence of various ions dissolved in cytosol (4,8,35,38–40). For a comprehensive overview of the ion effects, we conducted the gel mobility assay for the 15-kb plasmid DNA treated with 1.0 mM cisplatin in various buffer conditions (Supplementary Figure S4 and see Supplementary materials and methods for details). Compared with Cl^- (lanes 3–7 in Supplementary Figure S4B), carbonate and phosphate ions suppressed cisplatin binding to DNA more effectively (lanes 8–12 and 13–17 in Supplementary Figure S4B, respectively). Then, we also tested cisplatin binding to DNA in the 'cytosol-mimicking' buffer (the right of Supplementary Figure S4C), whose ionic composition is similar to that of cytosol (see Supplementary materials and methods). Again, binding of cisplatin (lanes 3–8 in the right of Supplementary Figure S4C) was effectively suppressed for all tested concentrations of cisplatin, similarly to the case of [NaCl] = 180 mM (lanes 3–8 in the left of Supplementary Figure S4C). As noted before (8), this suppression is likely due to competition of these ionic species with DNA for cisplatin binding, not to altered release of chloride from cisplatin. In any case, the inhibitory effect by cellular ions deserves proper attention, and it is uncertain whether the reduced cisplatin binding due to those cellular ions would be still sufficient to produce the observed cytotoxicity and anticancer effect if cisplatin mainly acts on bare DNA. Since chromatin, predominant form of DNA *in vivo*, plays crucial roles in various biological functions and can be a physicochemically disparate target to cisplatin, the chromatinic existence of DNA must be considered to understand the mechanism of cisplatin action *in vivo*. Thus, we investigated the effect of cisplatin on the N-DNA in 180 mM NaCl solution, which mimics the greatly compromised cisplatin binding inside living cells.

Mechanical behaviour of N-DNA

A nucleosome is the basic organizational unit of eukaryotic chromosome. The question is then how cisplatin affects the structural property of N-DNA. By crosslinking two distal segments of the same DNA strand or simply kinking DNA at multiple sites to snuggle a nucleosome core particle (NCP) stably, cisplatin may fasten the structure of N-DNA. Thus, we tested how cisplatin affects the stability of NCP using single-molecule measurements.

As a force-induced DNA melting process, the DNA overstretching transition (OST) has been extensively studied via single-molecule force spectroscopy measurements (41–47). We utilized the OST of N-DNA because it provided the excellent opportunity to access the rigidity and integrity of N-DNA. For experiments, we only used a nicked dsDNA to avoid any complication due to change in DNA superhelicity. Therefore, the OST of our bare DNA tethers occurred at $F \sim 65$ pN (Figures 2A, 3A and D), which is a typical onset force for OST (41,42). To induce a N-DNA assembly *in situ*, a tethered DNA molecule was first incubated with a buffer containing a mixture of histone-loading chaperone NAP1 (5 nM) and core histones (1.5 nM H3.1/H4 and 4 nM H2A/H2B) for 30 min inside the chamber. During buffer exchange and pre-incubation of protein complexes, the DNA tether was pulled at $F \sim 10$ pN to slow down the assembly reaction, preventing aberrant, immature histone-DNA aggregates. The N-DNA structure began to be assembled by decreasing $F < 1$ pN. When F was kept constant at 0.95 pN, the end-to-end distance of the DNA tether gradually decreased to 1.8 μm by assembling the N-DNA structure ($t = 0$ in Figure 2B), corresponding to ∼45% of the extension of the original DNA ($L \sim 4.2$ μm) at the same force ($t = 0$ in Figure 2A).

To check if the NCPs had been properly assembled, we analysed the time trace of DNA length during the period of NCP assembly and measured individual step sizes from the time trace (Supplementary Figure S5). To identify steps and get their details from a raw time-trace data acquired for 10 min at $F \sim 0.95$ pN (grey in Supplementary Figure S5A and B), we applied a step-detection algorithm developed by Arunajadai and Cheng (red lines in Supplementary Figure S5A and B) (48). We found a major peak at -25 ± 0.9 nm in the step histogram (Supplementary Figure S5C). Recalling that one turn of DNA around a histone octamer is about 25 nm long and descending and ascending steps correspond to DNA wrapping and unwrapping from histones, respectively (20,49,50), our observation confirms that nucleosomes had been properly assembled. This type of step-size analysis was used as a rule to judge the formation of NCP previously (20,21).

The N-DNA molecule prepared as such was stable and firm without being lengthened when the tether was pulled under 3 pN's tension. Assuming that histones associate with DNA only in the form of octamer and that octamers are fully wrapped by DNA in 1.7 turns (146 bp ∼ 50 nm), the number of nucleosomes (n) assembled onto this N-DNA is calculated by $n = (L_{DNA} - L_{N\text{-}DNA})/0.05 \sim 46$, where L_{DNA} and $L_{N\text{-}DNA}$ are the extensions of the original DNA (4.2 μm) and N-DNA (1.8 μm) measured at $F \sim 3$ pN, respectively.

After washing free histones out of the sample chamber with PBS buffer, we mechanically ruptured the assembled N-DNA by stretching it with a higher F as shown in the green boxed area in Figure 2B (also see its blown-up in Supplementary Figure S6A). Besides the unwrapping steps of 27.2 ± 0.4 nm in mean size, much larger steps, of 50–100 nm in size, were observed at even higher F ($20 < F < 40$ pN), indicating that multiple nucleosomes undergo DNA unwrapping simultaneously (Supplementary Figure S6C). At $F \sim 40$ pN, the DNA molecule restored its extension to 95% of that of bare DNA (Supplementary Figure S6A). This result is consistent with the previous report illustrating that the initial unlooping of DNA from histone cores was observed above $F \sim 3$ pN and then subsequent unwrapping events followed at higher force between 5 and 25 pN with a similar step size of 25 nm (20). We note that such a divergent distribution of rupturing force may originate from sequence heterogeneity in histone-wrapping DNA because the main part of our DNA tether originates from a 15-kb 'random' plasmid.

Another notable point in the force-extension measurement of N-DNA is that hysteresis exists in high-tension ($F > 60$ pN) as well as intermediate-tension ($3 < F < 20$ pN) regimes (Figure 2F). The hysteresis in the latter regime was reported previously (50–52) but the hysteresis in the higher force regime has not been explored for N-DNA. The fully unwrapped N-DNA at 40 pN exhibits the OST at $F \sim 70$ pN (point 'a' in Figure 2B and F), notably higher than ∼ 65 pN, level of force required for the OST in bare DNA at a mild salt condition (41,42). The elevated onset force suggests that some residual histones are still bound onto the DNA strand, stabilizing DNA duplex from base unstacking or denaturation, prerequisite for the OST. Indeed, some histone proteins remain associated even after N-DNA molecules are mechanically fully unwrapped, indicated by the fact that a reassembly of a fully unwrapped molecule (recovered from overstretching) to N-DNA is achieved in each relaxation run of stretching–relaxation (S–R) cycle for the same DNA molecule although a gradual, partial loss of histone octamers from DNA seemed to be inevitable cycle after cycle (53). The protein-induced elevation of the onset force for OST is not unusual as the OST onset force is elevated to ∼73 pN for HMGB-bound DNA molecules in the presence of the saturated concentration of HMGB (54). When this overstretched DNA molecule was relaxed, it behaved like bare DNA until F reduced to ∼1 pN. Below 1 pN, it was, however, collapsed because residual histones were reassembled to recover N-DNA partly as shown in the green box in Figure 2F (red trace in Supplementary Figure S7).

We then tested the effect of strong ionic condition on the N-DNA that had undergone the OST (or also on *de novo* N-DNA) shown in Figure 2B by changing buffer to 3 M NaCl solution. Immediately, the end-to-end distance of the reassembled N-DNA was restored to that of bare DNA, $L \sim 4.2$ μm at $F \sim 3$ pN (point 'a' in Figure 2C). Its S–R cycle (Figure 2G) showed a behaviour very similar to that of the original DNA in Figure 2E, except that the onset OST force was reduced to ∼60 pN (point 'b' in Figure 2C and G). This reduced onset force under strong ionic condition is consistent with earlier reports showing that high ionic conditions (say, >1 M NaCl) in fact destabilize DNA, resulting in a

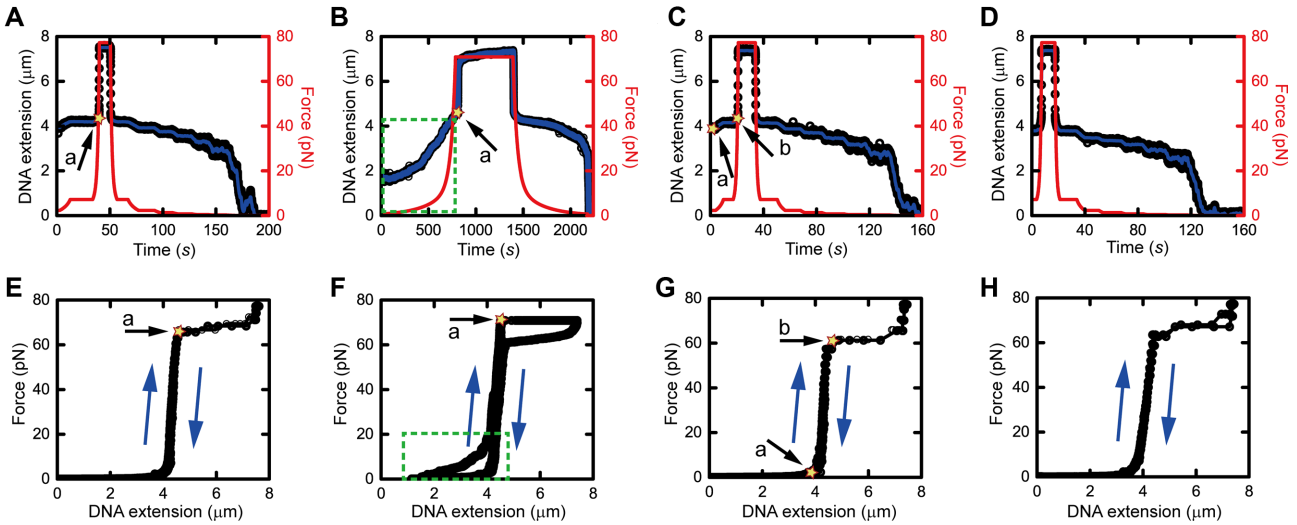

Figure 2. Force-extension behavior of a N-DNA molecule under various ionic conditions. (**A**, **E**) Typical response (raw extension data, black; extension data averaged over 1 s, blue) of a bare DNA in PBS solution with respect to varying tension (red) (A) and the force-extension curves from the S–R cycle driven by increase and decrease of tension (marked by upward and downward arrows, respectively) (E). The OST in a bare DNA happens at $F \sim 65$ pN (point 'a' in (A and E)). (**B**, **F**) Mechanical rupturing and relaxation of a N-DNA in PBS solution. Temporal extension of a N-DNA in a S–R cycle and the force-extension curves of the N-DNA are shown in (B and F), respectively. The curves clearly show the hysteresis. Here, the hysteresis appears in two different force regimes, high (60–75 pN) and intermediate (3–20 pN). (**C**, **G**) Salt-induced disassembly of a N-DNA via change of buffer to 3 M NaCl. Temporal extension (C) and the force–extension curves (G) of a N-DNA are acquired and displayed similarly to (B and F). The curves exhibit no hysteresis, similarly to the case of a bare DNA. This suggests that NCPs assembled onto DNA were fully disrupted by releasing histones into solution. Due to the high ionic strength, the onset force of OST was decreased to ~60 pN (point 'b' in (C, G)). (**D**, **H**) Response of a DNA (or N-DNA) recovered from the salt challenge. The buffer was restored to PBS. Temporal extension (D) and the force-extension curves (H) of DNA are acquired and displayed similarly to the above-mentioned data. This result confirms that there are no more residual histones on the DNA strand and the DNA is just like bare DNA shown in (E).

lower DNA melting temperature (55) while in the intermediate range, the presence of ions (<1 M NaCl) is beneficial to the stability of DNA double helix (32,56,57). To check if any residual histones were still bound to the DNA, we measured again its S–R cycle after replacing the chamber solution with PBS. We expected the DNA to be collapsed again under the mild ionic condition if any residual histones were still associated with the DNA. The DNA molecule, however, behaved like bare DNA this time (Figure 2D and H), indicating that histone proteins were finally and irreversibly all dissociated due to strong interference of abundant ions with electrostatic interaction between DNA and histones.

Efficient structural fixation of the N-DNA by cisplatin in 180 mM NaCl solution

Next, we investigated the effect of cisplatin on N-DNA. A N-DNA molecule prepared as above was incubated with 3.3 mM cisplatin in 180 mM NaCl solution with the molecule pulled at $F \sim 1$ pN. After washing free cisplatin out with PBS solution, we tried to pull the N-DNA molecule. As shown in Figure 3B, the condensed structure of N-DNA was stably retained although F increased up to ~90 pN, practical upper limit of applicable force to this molecule in our MT system. Even in the case that mechanical pulling was applied for synergy to wreck N-DNA in the presence of extreme ionic condition such as 3 M NaCl, its extension was never altered (Figure 3C). Such cisplatin-bound N-DNA (CBN-DNA) exhibits irreversible structural fixation by cisplatin crosslinking, indicating that tightly pinched nucleosomes are just frozen and cannot respond to external disturbances such as tension and salt challenge (red and blue curves in Figure 4A, measured in PBS and 3 M NaCl, respectively). We thus conclude that cisplatin can effectively fix the N-DNA by crosslinking multiple sites on the DNA segment that winds core histones. One notable point is that we did not observe the OST up to 90 pN in this CBN-DNA from the initially nicked DNA molecule. One plausible explanation for this is that DNA nicks (likely up to a few) happen to be in the part of DNA wrapped around histones and sequestered from torsion-responsive (bare) DNA segments upon cisplatin crosslinking (see case (a) in Figure 6C for schematic illustration). Thus, this CBN-DNA became torsionally constrained and supercoilable. In other cases, we observed the OST from CBN-DNA molecules treated with the same concentration of cisplatin (3.3 mM) because, in those cases, DNA nicks are located in DNA linker regions, resulting in torsionally unconstrained DNA (Supplementary Figure S8B, C, H, and I and case (b) of Figure 6C for schematic illustration). Indeed, it was previously reported that the OST onset force for nick-free DNA is the same as the one for nicked DNA if the nick-free DNA is torsionally unconstrained (58).

We next tested what would happen to N-DNA when it is incubated with a diluted cisplatin solution (Figures 3E and F and Supplementary Figure S8E, F, K and L). Surprisingly, the N-DNA was structurally fixed even with a very diluted cisplatin solution (~0.1 mM), comparable to a dose clinically used (>0.03 mM) (59) or locally measured (~0.04 mM) (2) in cancer chemotherapy (see the discussion about the clinical dose of cisplatin below). A N-DNA assembled to be 1.8 μm in extension was incubated with 0.1 mM cisplatin in 180 mM NaCl solution at $F \sim 1$ pN. Up to ~10 pN, its collapsed form remained unchanged

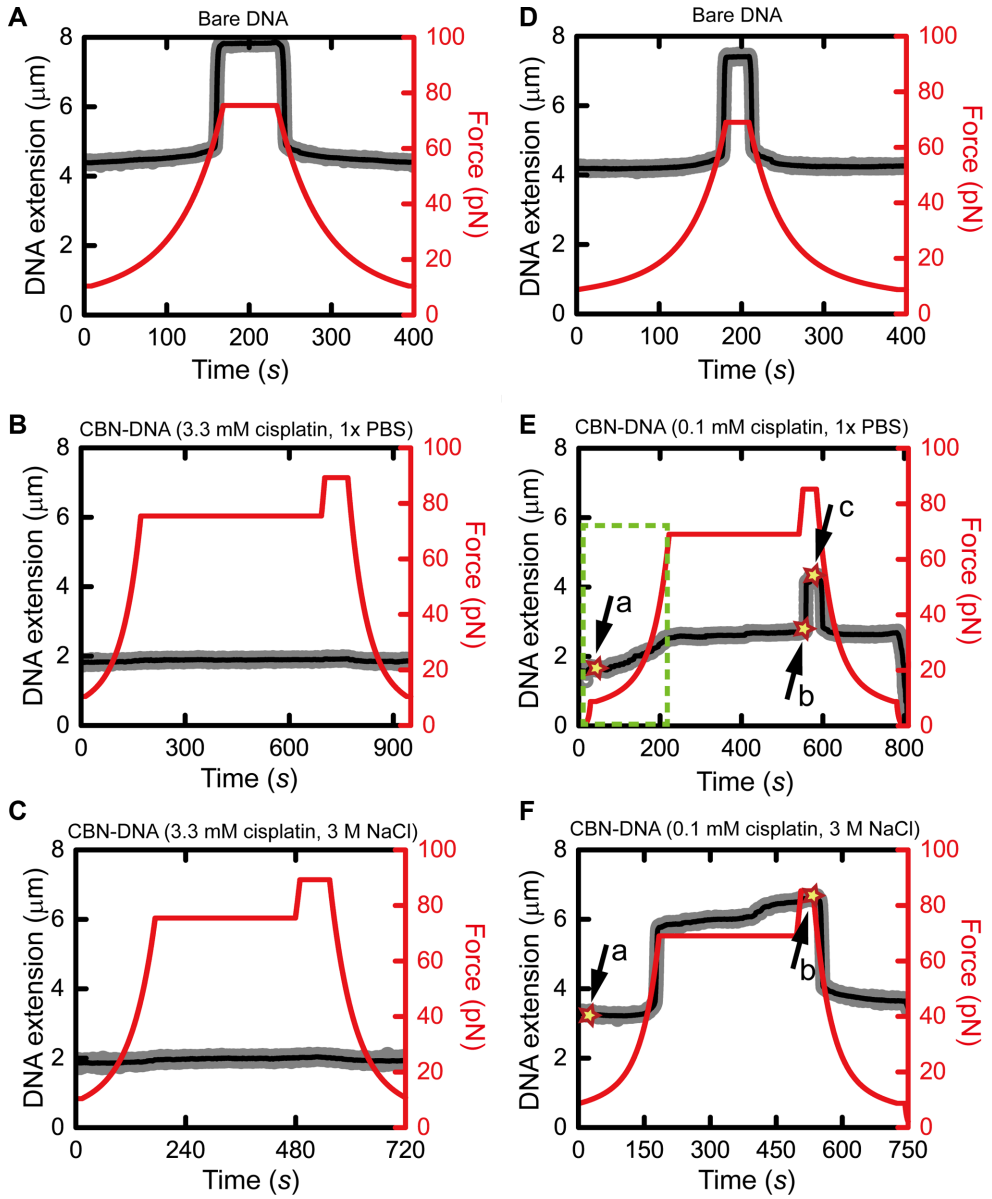

Figure 3. Physical change of single N-DNA molecules induced by cisplatin treatment. Here cisplatin was supplied at two different concentrations, (B, C) high (3.3 mM) and (E, F) low (0.1 mM), the latter being clinically relevant. (**A**) Temporal extension of a bare DNA (raw extension data, grey; extension data averaged over 0.5 s, black) with respect to varying tension (red). Because this DNA was nicked, its OST happened at $F \sim 65$ pN. (**B**, **C**) Constant extension of a CBN-DNA regardless of applied tension indicates the structural fixation of the N-DNA incubated with 3.3 mM cisplatin in PBS solution (B) and even after changing the solution to 3 M NaCl (C). Here, the N-DNA molecule in (B) was formed by incubating NAP1-associated core histones to the same bare DNA molecule in (A). (**D**) (A)-like data for another bare DNA used in (E and F). (**E**, **F**) Response of a N-DNA incubated with 0.1 mM cisplatin in PBS solution (E) and after changing the solution to 3 M NaCl (F). Panels from (B) to (F) follows the same convention used in panel (A).

(point 'a' in Figure 3E). Considering that its original extension was ∼4.1 μm (Figure 3D), this CBN-DNA had about 46 NCPs. Above $F \sim 10$ pN, this CBN-DNA was partly ruptured, showing stepwise elongation with the average step size of 20 ± 0.3 nm (green boxed area in Figure 3E and its corresponding blown-up in Supplementary Figure S9A). This elongation of CBN-DNA is similar to that of pristine N-DNA (Supplementary Figure S6), implying that some NCPs are not locked as in pristine N-DNA because of low cisplatin concentration and are easily unwrapped by tension.

While all NCPs in a pristine N-DNA would be disassembled by being pulled at $F \sim 40$ pN, this CBN-DNA has not been fully unwrapped and still exhibits stepwise lengthening to 2.6 μm beyond 40 pN (horizontal line drawn in Supplementary Figure S9A). Eventually, the CBN-DNA was lengthened by ∼0.8 μm as a result of force-induced rupturing of ∼20 cisplatin-exposed NCPs. The average step size measured from Supplementary Figure S9A was 20 ± 0.3 nm (Supplementary Figure S9B), slightly shorter than 25 nm, length of one turn of DNA in pristine N-DNA, indicating the possibility of imperfect DNA unwrapping due to cis-

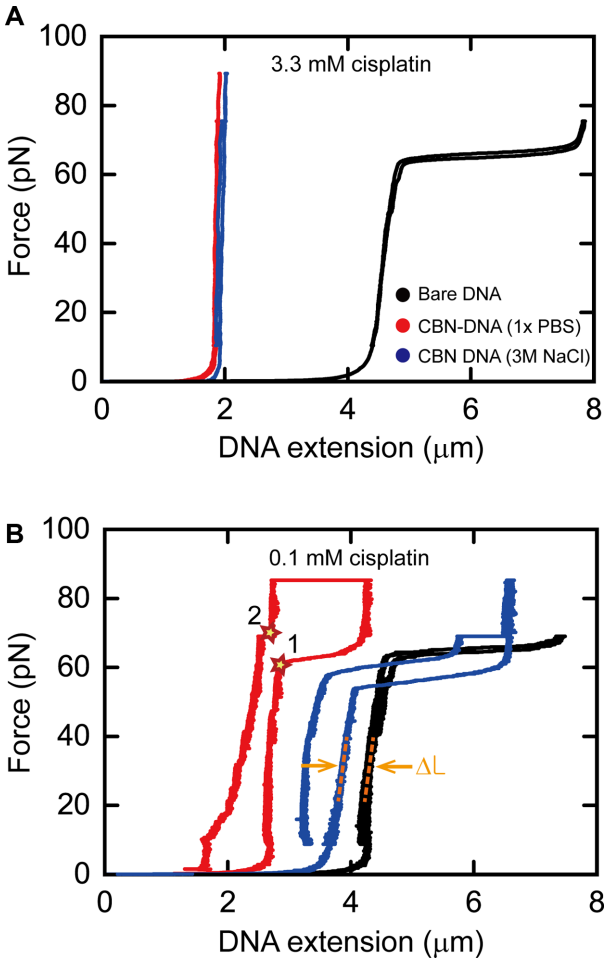

Figure 4. S-R cycles of the CBN-DNA molecules shown in Figure 3. (**A**) The collapsed form of CBN-DNA after 3.3 mM cisplatin treatment exhibited neither the OST nor the hysteresis in a mild (red) and extremely high salt condition (blue). A typical S-R cycle for a bare DNA was shown in black for comparison. (**B**) A CBN-DNA prepared with 0.1 mM cisplatin was stretched by mechanical force. The hysteresis is prominent in the CBN-DNA molecule both in a mild (red) solution and under the extremely high salt condition (blue). The maximum extensions of the CBN-DNA achieved upon OST in both PBS (red) and 3 M NaCl (blue) solutions were shorter than that of its original bare DNA (black).

platin crosslinking. Then, this extension of the CBN-DNA was stably maintained at ∼60 pN. At $F > 80$ pN, the OST took place (point 'b' in Figure 3E) and the extension of the CBN-DNA abruptly changed (point 'c' in Figure 3E). From the measured length of the unfastened DNA fraction (2.6 μm), we can calculate the post-OST extension of the CBN-DNA as $L_{\text{CBN-DNA}} \times 1.7 \sim 4.4$ μm, where 1.7 is the overstretching factor. This estimate is in good agreement with our experimental result ∼4.3 μm, measured at point 'c' in Figure 3E, indicating that the fastened part of DNA makes little contribution to the extension of DNA. In addition, histones (or disassembled octamers) associated with DNA by cisplatin crosslinking seem to boost the stability of DNA (as implied in Figure 2B and F) so that the OST onset force was significantly elevated to >80 pN. In the run of relaxation, a CBN-DNA, after overstretched, behaved somewhat like a bare DNA (but shorter). The S–R curve exhibited a large hysteresis, which likely arose from merging high-tension and intermediate-tension hystereses as shown in Figure 2F (red curve in Figure 4B). Upon recovery from the OST ('1' on red curve in Figure 4B), the CBN-DNA adopts the same extension as the maximum extension of the pre-OST CBN-DNA ('2' on the same red curve). It suggests that the DNA and N-DNA exposed to the clinical dose behave much like intact bare DNA and pristine N-DNA, respectively, except for a few fixed NCP by cisplatin binding.

When the CBN-DNA was exposed to 3 M NaCl, its extension increased from 2.6 μm to 3.3 μm at $F \sim 10$ pN (point 'a' in Figure 3F). Then, the molecule underwent the OST at $F \sim 60$ pN, similarly to a bare DNA under the same ionic condition. The salt-induced additional lengthening of the CBN-DNA is likely caused by partial dissociation of histone octamers in strong ionic environment, hinting at asymmetric DNA unwrapping from partially disassembled octamers, consistently with a recent study (60). Transient intermediate states in DNA-histone association have been revealed by time-resolved small-angle X-ray scattering method, illustrating how histone octamers could be dissociated into imperfect forms such as tetrasome or hexasome, accompanied by DNA partial opening or unwrapping in a salt-dependent manner. Despite the substantial interruption of self-organization of octamers and favourable interaction between DNA and histones, this DNA molecule remained shorter by ∼200 nm than the original DNA (see ΔL in Figure 4B) because part of DNA was still packaged with residual histones as shown in the relaxation run of bare and CBN-DNA in Figure 4B. Thus, we conclude that a few histones or some fragment of nucleosome are still engaged on the DNA. This experimental result illustrates that the clinical dose of cisplatin is still effectively working even in 180 mM NaCl solution.

In Supplementary Table S3, we provide a full list of data taken from 12 different DNA molecules that feature three states of DNA (bare DNA, N-DNA and CBN-DNA). Among them, three independent CBN-DNA molecules, #1's and #2-3's, are presented in Figure 3 and Supplementary Figure S8, respectively. The data all show fastening of chromatin by cisplatin in a dose-dependent manner. One can see that these data display heterogeneity even under the same experimental condition, which is quite natural in single-molecule assays. Most likely, such heterogeneous behaviours would arise from a different number and distribution of nucleosomes assembled on a long DNA tether with a random sequence.

Cisplatin effectively suppresses transcription from a chromatin template as revealed by the *in vitro* transcription assay

To facilitate gene expression *in vivo*, chromatin should be dynamically modified to a transcriptionally-active open conformation, in which genes are accessible by regulatory transcription factors. We then suppose that the structural fixation of chromatin by cisplatin may impair chromatin remodelling and thus suppress transcription. To confirm this hypothesis, we performed the *in vitro* transcription assay (Figure 5) with cisplatin-treated chromatin as schematized in Figure 5D and compared the efficiencies of transcription, that is, the amounts of RNA expressed from untreated

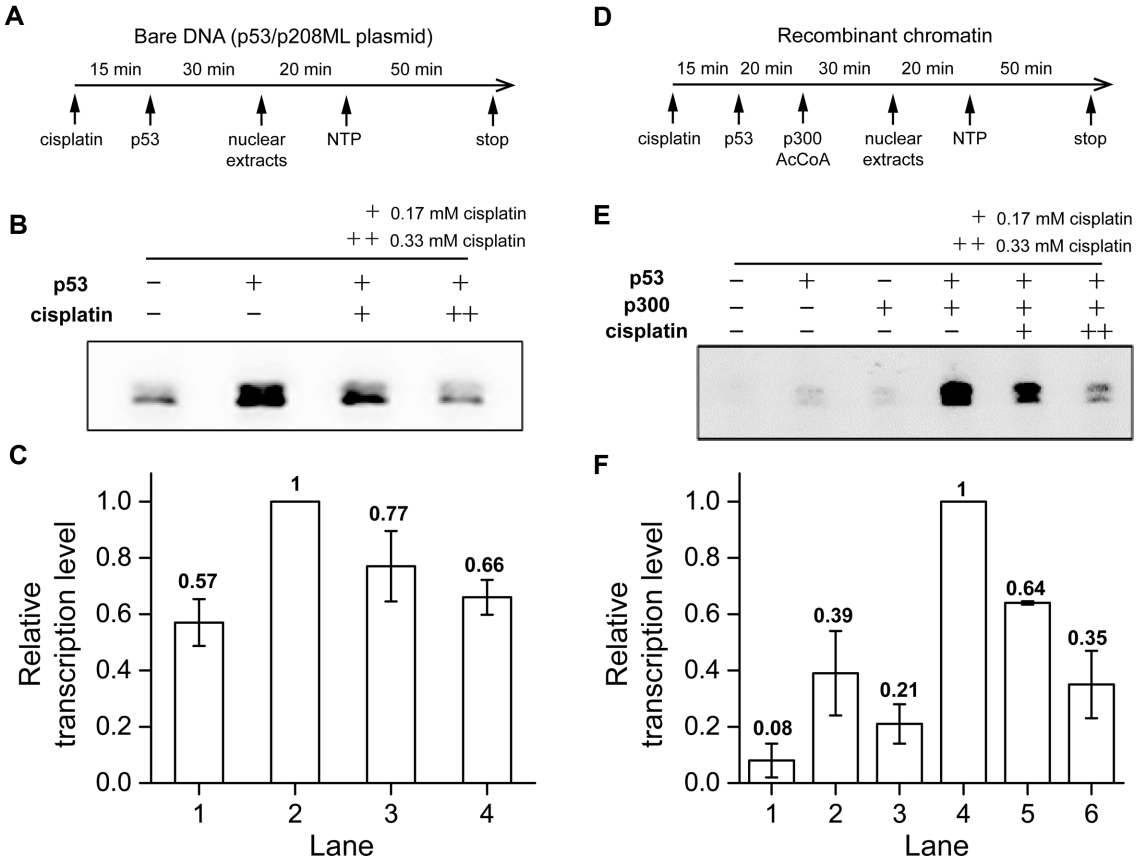

Figure 5. *In vitro* transcription from cisplatin-treated DNA and chromatin templates. (**A**, **D**) Schematic representation of the *in vitro* transcription assay with cisplatin-treated (A) DNA and (D) chromatin. Bare DNA and reconstituted chromatin were treated sequentially with cisplatin, transcription factors (p53 for bare DNA; p53, p300 and AcCoA (acetyl coenzyme A) for chromatin), nuclear extracts derived from HeLa cells, and NTP in the indicated order and time. (**B**, **E**) Effect of cisplatin on *in vitro* transcription from bare DNA (B) and chromatin templates (E). Reaction conditions of each lane are indicated above the lane. (**C**, **F**) Relative transcription levels were quantitated by phosphorimager and normalized to that of p53-dependent transcription for bare DNA and p53- and p300-dependent transcription for chromatin (lane 2 in (C) and lane 4 in (F), respectively). The error bars in histograms represent the standard deviation of data in triplicates.

and cisplatin-treated chromatins. For proper function, eukaryotic RNA polymerases extracted from nuclei require transcription factors, which bind to a promoter DNA and regulate the transcription activity (61,62). Indeed, the transcription activity on bare DNA in the absence of p53 (lane 1 in Figure 5B and C) was reduced to 57% compared to the control experiment with p53 (lane 2 in Figure 5B and C). Transcription inhibition was more pronounced for N-DNA substrates, amounting to about 92% inhibition in the absence of both p300 and p53 (lane 1 in Figure 5E and F) and 61% or 79% inhibition in the absence of either p300 or p53 (lanes 2, 3 in Figure 5E and F). Then, we investigated the effect of cisplatin on transcription, that is, transcription inhibition induced by cisplatin treatment to bare and N-DNA substrates. Although the level of transcription was decreased by cisplatin treatment for both DNA substrates, N-DNA substrates exhibit larger transcription inhibition than bare DNA substrates: for 0.17- and 0.33-mM cisplatin treatment, N-DNA displayed 1.5 (lane 3 in Figure 5C lane 5 in Figure 5F) and 1.9 (lane 4 in Figure 5C and lane 6 in Figure 5F) times more transcription inhibition than bare DNA, respectively. This finding supports our picture that the structural fastening of chromatin by cisplatin impairs essential gene expressions, leading to cytotoxicity required for anti-cancer activity.

In a previous report, Todd and Lippard reported that gene transcription was suppressed similarly in both bare DNA and N-DNA upon cisplatin treatment (63). They concluded that cisplatin interferes with gene transcription regardless of the existence of N-DNA. They, however, used a special short DNA (204 bp) with one pre-formed cisplatin-DNA adduct in the middle and prepared a mononucleosome from it. In such a case, reactive cisplatin is absent during or after nucleosome assembly. In order to reveal directly how active cisplatin attacks N-DNA molecules and alters the transcription efficiency of the N-DNA templates, we administrated cisplatin to an enzymatically-formed N-DNA molecule with a long random sequence (5.4 kb). While Todd and Lippard performed *in vitro* transcription assays by using purified T7 RNA polymerases and the short DNA with a T7 promoter, not with enzymes from eukaryotic cells, we conducted *in vitro* transcription assays with nuclear extracts from eukaryotic cell to mimic *in vivo* transcription. Our experimental setting represents *in vivo* situations better to reveal altered transcription activity due to the formation of cisplatin adducts.

DISCUSSION

The anti-cancer effect of cisplatin has been elucidated mainly in the context of the standard model, in which cisplatin is activated in the Cl^- poor cellular environment and generates DNA lesions by crosslinking two neighbouring purine bases, largely overlooking the effect of DNA packaging by histones. Over years, it has been shown that cellular anions besides Cl^- can compete with the N7 of purines for cisplatin binding and histones can be trapped by cisplatin-bound DNA strands (13,15). Only cisplatin that avoids association with abundant cellular ions finds their way to DNA and the toxicity must arise from the surviving cisplatin to successfully attack the target molecules (64). Thus, cisplatin binding on the target might be a rare event in the cellular environment crowded with an enormous number of competitors. Therefore, it is natural to ask whether (bare) DNA would be the (only) target of cisplatin for currently observed strong cytotoxicity of cisplatin or there are other more vulnerable targets. It was not until recently that the importance of the effects by cellular ions and histones came into light (7,13–15). We hypothesized that cisplatin binding to chromatin, not bare DNA, would be more deleterious to cell's normal metabolism. To address the effect of DNA packaging on cisplatin's drug efficacy, we examined the effect of nucleosome formation on DNA damage by cisplatin by measuring the mechanical property of N-DNA molecules and the *in vitro* transcription through chromatin before and after cisplatin binding.

From the gel assay, we confirmed that cisplatin binding is suppressed not only by ambient Cl^-, but also by other anions (phosphate and carbonate) and cations (Na^+ and K^+) common in cells. From the systematic comparison, we then estimated relative abilities of these ions to suppress cisplatin binding. We showed that the suppressive effects of these ions are comparable to that of Cl^- which is rather unexpected, although the effects by cellular anions were addressed in previous reports (4,8,40). In order to project our result towards the *in vivo* situation, we tested cisplatin activity in the 'cytosol-mimicking' buffer and observed the suppression of cisplatin binding similar to the case of [NaCl] = 180 mM. Thus, the cellular condition for the reduced cisplatin binding can be mimicked simply by using 180 mM NaCl solution for the single-molecule manipulation assays.

In this paper, we would provide a complementary mechanism within the standard picture to augment the anti-cancer effect by cisplatin. As DNA mainly exists in the form of chromatin, we tested the effect of cisplatin on the assembled N-DNA. First, the treatment of 3.3 mM cisplatin induced dramatic structural changes in, here structural fixation of, the NCPs in the assembled N-DNA even in high-chloride salt conditions. Second, to our surprise, we found that a much less dose (0.1 mM) of cisplatin, relevant to a clinical one, suppresses the release of core histones from DNA by mechanical force or salt challenge, though not as much as in the sample treated with 3.3 mM cisplatin. Moreover, by the *in vitro* transcription assay with chromatin templates, we showed that the structural fixation of chromatin by cisplatin indeed suppressed transcription of a gene within the locked chromatin. Thus, we conclude that cisplatin-chromatin adducts would impair chromatin remodelling required for normal gene expression as well as repair of DNA lesion, which likely constitutes the effective mechanism for cytotoxicity by cisplatin.

A comment on the clinical dose of cisplatin should be made in order. The amount of cisplatin adducts formed in the MT assay with the lower dose of cisplatin (0.1 mM) in 180 mM NaCl could be still higher than that in cell/tissue assays conducted with the same dose of applied cisplatin, where cisplatin binding to DNA is significantly reduced by various competing factors in cells and dilution of cisplatin occurs during delivery or by efflux. Considering the low frequency of bound cisplatin in cellular DNA (1 Pt per 100 000 $\sim$ 500 000 nt) (64), one may expect to have one locked nucleosome out of 1000 nucleosomes. There are however numerous nucleosomes in each human cell ($>10^7$ from simple estimation) and thus about 10,000 locked nucleosomes. Only counting the nucleosomes within genes (1 or 2% of human genome), we surely have several hundreds of locked nucleosomes positioned in genes. It cannot be ruled out that locked nucleosomes in non-coding regions also cause cytotoxic effects. If one considers only active genes or critical genes responsible for cell fate or survival, this number would be reduced further. It is however clear that a considerable number of nucleosomes within active genes in each cell are affected by cisplatin binding and their transcription can be switched off or significantly compromised by the binding. Thus, it is no doubt that cisplatin binding (to N-DNA) in clinical treatment would make significant impacts on cell fate. Given the low binding frequency of cisplatin in the *in vivo* situation, we may have no cisplatin adduct within the short DNA tether or one at most at such a low binding rate. Even if there are a few, it may not be easy to detect N-DNA locking. Thus, in our assay, the fraction of locked N-DNA is somewhat exaggerated not because we believe it is quantitatively the case in cells but simply because we want to detect locked N-DNAs (and find the evidence of N-DNA locking under our experimental sensitivity). Our observation made for concentrated CBN-DNA does not weaken our conclusion to any extent as noted above.

Figure 6 summarizes the proposed mechanism of the anti-cancer effect of cisplatin via its fastening of chromatin proposed from our experimental results. A N-DNA assembled with NAP1 forms a well-ordered nucleosomal array (Figure 6A). Such NCPs could be mechanically disrupted by applied force (typically, higher than 20 pN), but a portion of histones remain bound on DNA (yellow circle in Figure 6B) as revealed by the elevated OST onset force ($\sim$70 pN; Figure 2B and F) in a N-DNA (3rd in Figure 6B). Such residual histones could be fully dissociated by changing buffer to 3 M NaCl solution even under a low stretching force of $\sim$3 pN (last in Figure 6B). When N-DNA molecules are treated with cisplatin, their mechanical properties are dramatically altered. CBN-DNA is tough against applied tension and high ionic strength. The extreme rigidity of CBN-DNA provides critical insights into the mechanical effect of histones on chromatin and the hallmark of modifications of chromatin by cisplatin. NCPs fixed completely by cisplatin (red circles in Figure 6C) are mechanically inert against strong tension beyond the OST onset force as well as ionic disturbance. The occurrence of OST in our assay depends on the location of a DNA nick (red arrows). If a

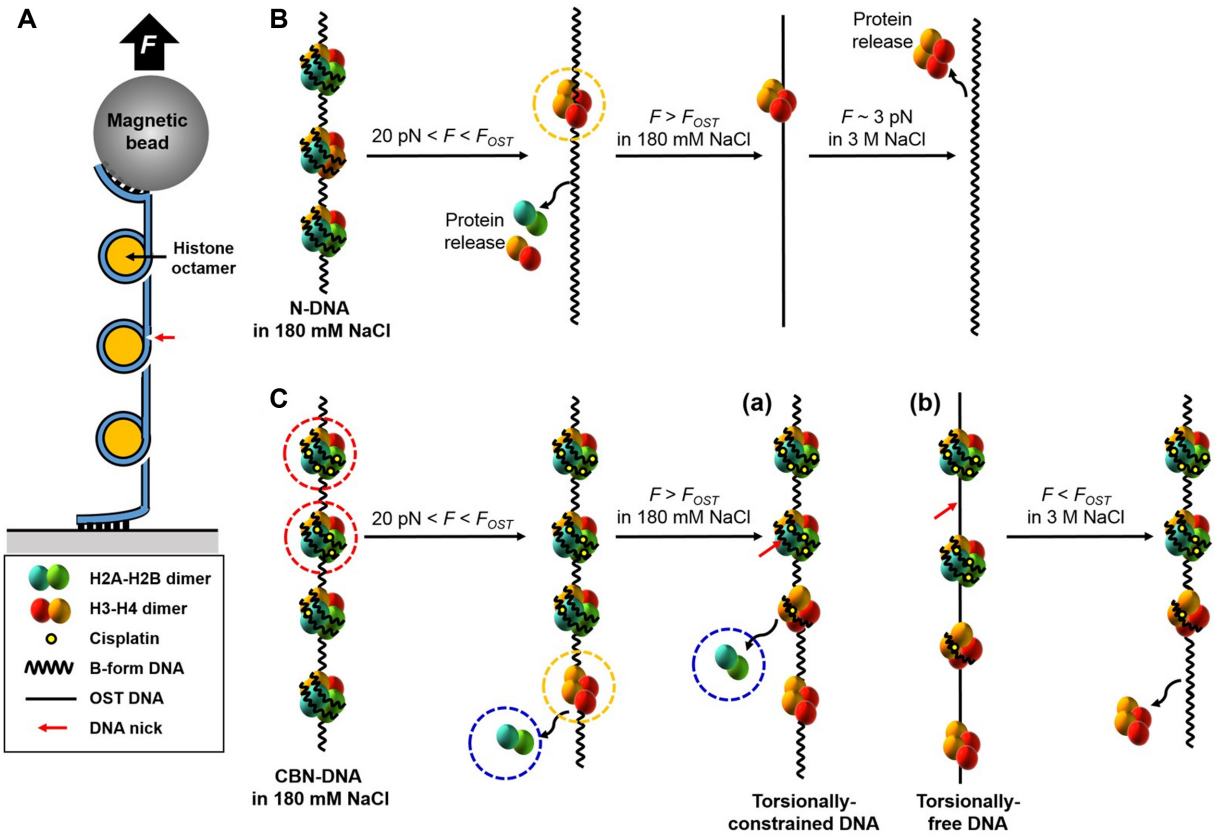

Figure 6. Proposed mechanism of cisplatin's drug efficacy by chromatin fastening. (**A**) Cartoon of a N-DNA bearing several NCPs. (**B**) NCPs are mechanically disrupted by force, but lingering association of residual histones (yellow circle) is evident from the elevated level of OST onset force of ∼70 pN. Strong 3 M NaCl solution is capable of stripping N-DNA of core histones. (**C**) Structural fixation and modification of cisplatin-treated chromatin revealed by mechanical and ionic disturbances. Depending on the location of DNA nicks (red arrows), the OST may not be observed in our experimental setting (typically, maximum force applicable ∼100 pN) as shown in case (a) (case (a): DNA nicks hidden within cisplatin-fixed NCPs, and case (b): DNA nicks exposed in DNA linkers). The yellow, blue, and red circles indicate residual, released (cisplatin-free or loosely captured), and cisplatin-crosslinked histones, respectively.

nick is absent in linker regions and hidden within cisplatin-fixed NCPs, the OST would not be observed (case (a) in Figure 6C) as shown in our experimental results (Figure 3B and C). On the other hand, a CBN-DNA would behave like a torsionally-free DNA and exhibit the OST when nicks are located in DNA linker regions (case (b) in Figure 6C) as in Figure 3E and F. When N-DNA molecules are treated with cisplatin at low concentration, CBN-DNA is loosely fastened because NCPs are crosslinked partially and some NCPs are free of cisplatin. Such a CBN-DNA is gradually lengthened by applied force because partially crosslinked or cisplatin-free NCPs are disrupted (blue circles in Figure 6C). When a CBN-DNA is exposed to high NaCl solution, NCPs may be further taken apart, resulting in additional lengthening. However, even after overstretched in 3 M NaCl, a CBN-DNA may still bear a few NCPs fixed by permanent crosslinking of DNA (red circles in Figure 6C). Cisplatin-induced structural fixation of chromatin described here is dose dependent: the CBN-DNA prepared with a high concentration of cisplatin (e.g., 3.3 mM) tends to be fixed more tightly, have a shorter recovered extension after 3 M NaCl washing, and often lack OST compared to the counterpart prepared with a low concentration of cisplatin (e.g., 0.1 mM). Even in the latter case, it is clear that chromatin is mechanically and permanently fastened.

In the previous AFM study (28) as well as our MT measurement on bare DNA (Supplementary Figure S3), it was revealed that cisplatin can capture a loop of DNA, resulting in a drastic DNA condensation. Although both experiments suggested binding of cisplatin to two distal segments of DNA, which might trap a nucleosome irreversibly if this binding happens at the entry/exit sites of a nucleosome, the methods used in those assays could not be able to specify the position of cisplatin binding, and such binding sites on nucleosomes when applied to N-DNA. There is one intriguing possibility of enhanced cisplatin reactivity in the vicinity of a nucleosome (65–68). Histones have cysteine and methionine residues that contain sulphur. From the hard-soft acid base theory, platinum, a soft acid, prefers soft bases such as sulphide for complex formation to hard bases such as Cl^- and H_2O. Thus, cisplatin could be trapped by those residues and accumulated near the DNA-histone interface by forming a Pt–S bond. In the sulphur-bound Pt species, the ligand trans to the sulphur could be labilised (65–68), so cisplatin bound to a histone can be bound to a nitrogen on a nearby DNA base, leading to chromatin fastening. In fact, cisplatin was shown to bind with methio-

nine, and methionine-bound cisplatin can form a protein-cisplatin-DNA ternary complex. Our current understanding of cisplatin-induced chromatin fastening is limited for the following reasons: (i) usage of a long (∼12 kb) DNA molecule with a string of ∼50 nucleosomes, which obscures cisplatin-induced structural modifications at individual nucleosomes, and (ii) no structural information of preferential sites for cisplatin binding at the level of nucleosome. Therefore, structural biology assays such as X-ray crystallography or NMR might be of help to gather some missing information in order to dissect the phenomenon of cisplatin-induced nucleosome-fastening.

Our observations are consistent with a previous X-ray crystallographic and biochemical investigation illustrating the unexpected role of histone octamers, that is, reservoir of cisplatin. In the model, histones facilitate the transfer and thus binding of cisplatin to DNA, leading to the suppression of nucleosome mobility (14,15). An analogous view on the effect of cisplatin binding on NCP was also given previously (13). These previous findings strengthen our picture for the strong anti-cancer effect of cisplatin in two ways. First, cisplatin binding is more efficient near NCP than elsewhere, and the cisplatin bound at the crevice between DNA and histones may not be removed by the DNA repair machinery due to its impaired accessibility. This can aggravate the damages done by cisplatin. Second, by crosslinking DNA strands around NCP as inferred from both gel assay (15) and our single-molecule measurements, the dynamic nucleosome remodelling (dynamic engagement and disengagement of histones) is prohibited (see the schematic picture in Figure 6). Since such dynamic rearrangements of nucleosome structures are critical to most biological phenomena such as DNA replication, transcription, and repair (60,69), fastening of nucleosomes cannot be tolerated and may trigger all sorts of devastating outcomes. The apoptosis triggered by cisplatin-modified nucleosome will lead to clinical benefits as it will preferentially remove proliferating cancer cells. Our work is the first direct and unambiguous verification of cisplatin-induced irreversible fastening of nucleosome structure. The mechanical details gained at single molecule level here certainly clarifies the mechanism for the anti-cancer effect of cisplatin and would aid the development of improved agents and therapeutic tactics.

DATA AVAILABILITY

The data that support the findings of this study are available from the corresponding author upon reasonable request.

SUPPLEMENTARY DATA

Supplementary Data are available at NAR Online.

FUNDING

IBS-R023-D1 and NRF-2019R1A2C1089808 (to S.-C. H.); Global Research & Development Center Program [2018K1A4A3A01064272 to S.-C.H.] through the NRF funded by the Ministry of Science and ICT; NRF-2019R1A2C2090830 (to J. K.). Funding for open access charge: NRF-2019R1A2C1089808.

Conflict of interest statement. None declared.

REFERENCES

1. Wong,E. and Giandomenico,C.M. (1999) Current status of platinum-based antitumor drugs. *Chem. Rev.*, **99**, 2451–2466.
2. Boulikas,T. and Vougiouka,M. (2003) Cisplatin and platinum drugs at the molecular level. *Oncol. Rep.*, **10**, 1663–1682.
3. Siddik,Z.H. (2003) Cisplatin: mode of cytotoxic action and molecular basis of resistance. *Oncogene*, **22**, 7265–7279.
4. Jung,Y. and Lippard,S.J. (2007) Direct cellular responses to platinum-induced DNA damage. *Chem. Rev.*, **107**, 1387–1407.
5. Dabrowiak,J.C. (2009) In: *Metals in Medicine*. Wiley-Blackwell, Oxford.
6. Dasari,S. and Tchounwou,P.B. (2014) Cisplatin in cancer therapy: molecular mechanisms of action. *Eur. J. Pharmacol.*, **740**, 364–378.
7. Wang,D., Hara,R., Singh,G., Sancar,A. and Lippard,S.J. (2003) Nucleotide excision repair from site-specifically platinum-modified nucleosomes. *Biochemistry*, **42**, 6747–6753.
8. Binter,A., Goodisman,J. and Dabrowiak,J.C. (2006) Formation of monofunctional cisplatin-DNA adducts in carbonate buffer. *J. Inorg. Biochem.*, **100**, 1219–1224.
9. Bertini,I., Gray,H.B., Lippard,S.J. and Valentine,J.S. (1994) In: *Bioinorganic Chemistry. University Science Books*. Mill Valley, CA.
10. Mymryk,J.S., Zaniewski,E. and Archer,T.K. (1995) Cisplatin inhibits chromatin remodeling, transcription factor binding, and transcription from the mouse mammary tumor virus promoter in vivo. *Proc. Natl. Acad. Sci. U.S.A.*, **92**, 2076–2080.
11. Kim,M.S., Blake,M., Baek,J.H., Kohlhagen,G., Pommier,Y. and Carrier,F. (2003) Inhibition of histone deacetylase increases cytotoxicity to anticancer drugs targeting DNA. *Cancer Res.*, **63**, 7291–7300.
12. Wang,D. and Lippard,S.J. (2004) Cisplatin-induced post-translational modification of histones H3 and H4. *J. Biol. Chem.*, **279**, 20622–20625.
13. Danford,A.J., Wang,D., Wang,Q., Tullius,T.D. and Lippard,S.J. (2005) Platinum anticancer drug damage enforces a particular rotational setting of DNA in nucleosomes. *Proc. Natl. Acad. Sci. U.S.A.*, **102**, 12311–12316.
14. Wu,B., Dröge,P. and Davey,C.A. (2008) Site selectivity of platinum anticancer therapeutics. *Nat. Chem. Biol.*, **4**, 110–112.
15. Wu,B. and Davey,C.A. (2008) Platinum drug adduct formation in the nucleosome core alters nucleosome mobility but not positioning. *Chem. Biol.*, **15**, 1023–1028.
16. Lee,I.B. (2018) Developments of nanometry techniques and their applications towards physical characterization of nanoparticles and nucleic acids. Ph.D. Thesis, Korea University.
17. Eeftens,J.M., van der Torre,J., Burnham,D.R. and Dekker,C. (2015) Copper-free click chemistry for attachment of biomolecules in magnetic tweezers. *BMC Biophys.*, **8**, 9.
18. An,W., Palhan,V.B., Karymov,M.A., Leuba,S.H. and Roeder,R.G. (2002) Selective requirements for histone H3 and H4 N termini in p300-dependent transcriptional activation from chromatin. *Mol. Cell*, **9**, 811–821.
19. Petesch,S.J. and Lis,J.T. (2012) Overcoming the nucleosome barrier during transcript elongation. *Trends Genet.*, **28**, 285–294.
20. Vlijm,R., Smitshuijzen,J.S.J., Lusser,A. and Dekker,C. (2012) NAP1-assisted nucleosome assembly on DNA measured in real time by single-molecule magnetic tweezers. *PLoS One*, **7**, e46306.
21. Kim,S.H., Vlijm,R., van der Torre,J., Dalal,Y. and Dekker,C. (2016) CENP-A and H3 nucleosomes display a similar stability to force-mediated disassembly. *PLoS One*, **11**, e0165078.
22. Kim,J., Guermah,M. and Roeder,R.G. (2010) The human PAF1 complex acts in chromatin transcription elongation both independently and cooperatively with SII/TFIIS. *Cell*, **140**, 491–503.
23. te Velthuis,A.J.W., Kerssemakers,J.W.J., Lipfert,J. and Dekker,N.H. (2010) Quantitative guidelines for force calibration through spectral analysis of magnetic tweezers data. *Biophys. J.*, **99**, 1292–1302.
24. Bustamante,C., Marko,J.F., Siggia,E.D. and Smith,S. (1994) Entropic elasticity of λ-Phage DNA. *Science*, **265**, 1599–1600.
25. Lee,N.-K., Park,J.-S., Johner,A., Obukhov,S., Hyon,J.Y., Lee,K.J. and Hong,S.-C. (2008) Elasticity of cisplatin-bound DNA reveals the degree of cisplatin binding. *Phys. Rev. Lett.*, **101**, 248101.

26. Lee,N.-K., Park,J.-S., Johner,A., Obukhov,S., Hyon,J.Y., Lee,K.J. and Hong,S.-C. (2009) Investigation of the elasticity of a cisplatin-DNA adduct via single-molecule measurements and bimodal modeling. *Phys. Rev. E*, **79**, 041921.
27. Salerno,D., Brogioli,D., Cassina,V., Turchi,D., Beretta,G.L., Seruggia,D., Ziano,R., Zunino,F. and Mantegazza,F. (2010) Magnetic tweezers measurements of the nanomechanical properties of DNA in the presence of drugs. *Nucleic Acids Res.*, **38**, 7089–7099.
28. Hou,X.-M., Zhang,X.-H., Wei,K.-J., Ji,C., Dou,S.-X., Wang,W.-C., Li,M. and Wang,P.-Y. (2009) Cisplatin induces loop structures and condensation of single DNA molecules. *Nucleic Acids Res.*, **37**, 1400–1410.
29. Rocha,M.S. (2015) Extracting physical chemistry from mechanics: a new approach to investigate DNA interactions with drugs and proteins in single molecule experiments. *Integr. Biol.*, **7**, 967–986.
30. Oliveira,L. and Rocha,M.S. (2017) Force spectroscopy unravels the role of ionic strength on DNA-cisplatin interaction: Modulating the binding parameters. *Phys. Rev. E*, **96**, 032408.
31. Salerno,D., Beretta,G.L., Zanchetta,G., Brioschi,S., Cristofalo,M., Missana,N., Nardo,L., Cassina,V., Tempestini,A., Giovannoni,R. *et al.* (2016) Platinum-based drugs and DNA interactions studied by single-molecule and bulk measurements. *Biophys. J.*, **110**, 2151–2161.
32. Wenner,J.R., Williams,M.C., Rouzina,I. and Bloomfield,V.A. (2002) Salt dependence of the elasticity and overstretching transition of single DNA molecules. *Biophys. J.*, **82**, 3160–3169.
33. Baumann,C.G., Smith,S.B., Bloomfield,V.A. and Bustamante,C. (1997) Ionic effects on the elasticity of single DNA molecules. *Proc. Natl. Acad. Sci. U.S.A.*, **94**, 6185–6190.
34. Herrero-Galán,E., Fuentes-Perez,M.E., Carrasco,C., Valpuesta,J.M., Carrascosa,J.L., Moreno-Herrero,F. and Arias-Gonzalez,J.R. (2013) Mechanical identities of RNA and DNA double helices unveiled at the single-molecule level. *J. Am. Chem. Soc.*, **135**, 122–131.
35. Park,J.-S., Kim,S.H., Lee,N.-K., Lee,K.J. and Hong,S.-C. (2012) In situ analysis of cisplatin binding to DNA: the effects of physiological ionic conditions. *Phys. Chem. Chem. Phys.*, **14**, 3128–3133.
36. Skoko,D., Yan,J., Johnson,R.C. and Marko,J.F. (2005) Low-force DNA condensation and discontinuous high-force decondensation reveal a loop-stabilizing function of the protein Fis. *Phys. Rev. Lett.*, **95**, 208101.
37. Sankararaman,S. and Marko,J.F. (2005) Formation of loops in DNA under tension. *Phys. Rev. E*, **71**, 021911.
38. Tognella,S. (1990) Pharmacological interventions to reduce platinum-induced toxicity. *Cancer Treat. Rev.*, **17**, 139–142.
39. Hägerlöf,M., Papsai,P., Chow,C.S. and Elmroth,S.K.C. (2006) More pronounced salt dependence and higher reactivity for platination of the hairpin r(CGCGUUGUUCGCG) compared with d(CGCGTTGTTCGCG). *J. Biol. Inorg. Chem.*, **11**, 974–990.
40. Centerwall,C.R., Goodisman,J., Kerwood,D.J. and Dabrowiak,J.C. (2005) Cisplatin carbonato complexes. Implications for uptake, antitumor properties, and toxicity. *J. Am. Chem. Soc.*, **127**, 12768–12769.
41. Smith,S.B., Cui,Y. and Bustamante,C. (1996) Overstretching B-DNA: The elastic response of individual double-stranded and single-stranded DNA molecules. *Science*, **271**, 795–799.
42. Cluzel,P., Lebrun,A., Heller,C., Lavery,R., Viovy,J.-L., Chatenay,D. and Caron,F. (1996) DNA: An extensible molecule. *Science*, **271**, 792–794.
43. Fu,H., Chen,H., Marko,J.F. and Yan,J. (2010) Two distinct overstretching DNA states. *Nucleic. Acids. Res.*, **38**, 5594–5600.
44. Fu,H., Chen,H., Zhang,X., Qu,Y., Marko,J.F. and Yan.,J. (2011) Transition dynamics and selection of the distinct S-DNA and strand unpeeling modes of double helix overstretching. *Nucleic Acids Res.*, **39**, 3473–3481.
45. King,G.A., Gross,P., Bockelmann,U., Modesti,M., Wuite,G.J.L. and Peterman,E.J.G. (2013) Revealing the competition between peeled ssDNA, melting bubbles, and S-DNA during DNA overstretching using fluorescence microscopy. *Proc. Natl. Acad. Sci. U.S.A.*, **110**, 3859–3864.
46. Zhang,X., Chen,H., Fu,H., Doyle,P.S. and Yan,J. (2012) Two distinct overstretching DNA structures revealed by single-molecule thermodynamics measurements, *Proc. Natl. Acad. Sci. U.S.A.*, **109**, 8103–8108.
47. Zhang,X., Chen,H., Le,S., Rouzina,I., Doyle,P.S. and Yan,J. (2013) Revealing the competition between peeled ssDNA, melting bubbles, and S-DNA during DNA overstretching by single-molecule calorimetry. *Proc. Natl. Acad. Sci. U.S.A.*, **110**, 3865–3870.
48. Arunajadai,S.G. and Cheng,W. (2013) Step detection in single-molecule real time trajectories embedded in correlated noise. *PLoS One*, **8**, e59279.
49. Chien,F.T. and van der Heijden,T. (2014) Characterization of nucleosome unwrapping within chromatin fibers using magnetic tweezers. *Biophys. J.*, **107**, 373–383.
50. Cui,Y. and Bustamante,C. (2000) Pulling a single chromatin fiber reveals the forces that maintain its higher-order structure. *Proc. Natl. Acad. Sci. U.S.A.*, **97**, 127–132.
51. Bennink,M.L., Leuba,S.H., Leon,G.H., Zlatanova,J., de Grooth,B.G. and Greve,J. (2001) Unfolding individual nucleosomes by stretching single chromatin fibers with optical tweezers. *Nat. Struct. Biol.*, **8**, 606–610.
52. Meng,H., Andresen,K. and van Noort,J. (2015) Quantitative analysis of single-molecule force spectroscopy on folded chromatin fibers. *Nucleic Acids Res.*, **43**, 3578–3590.
53. Brower-Toland,B.D., Smith,C.L., Yeh,R.C., Lis,J.T., Peterson,C.L. and Wang,M.D. (2002) Mechanical disruption of individual nucleosomes reveals a reversible multistage release of DNA. *Proc. Natl. Acad. Sci. U.S.A.*, **99**, 1960–1965.
54. McCauley,M.J., Rueter,E.M., Rouzina,I., Maher,L.J. III and Williams,M.C. (2013) Single-molecule kinetics reveal microscopic mechanism by which high-mobility group B proteins alter DNA flexibility. *Nucleic Acids Res.*, **41**, 167–181.
55. Khimji,I., Shin,J. and Liu,J. (2013) DNA duplex stabilization in crowded polyanion solutions. *Chem. Commun.*, **49**, 1306–1308.
56. Punkkinen,O., Hansen,P.L., Miao,L. and Vattulainen,I. (2005) DNA overstretching transition: ionic strength effects. *Biophys. J.*, **89**, 967–978.
57. Zhang,X., Qu,Y., Chen,H., Rouzina,I., Zhang,S., Doyle,P.S. and Yan,J. (2014) Interconversion between three overstretched DNA structures. *J. Am. Chem. Soc.*, **136**, 16073–16080.
58. Paik,D.H. and Perkins,T.T. (2011) Overstretching DNA at 65 pN does not require peeling from free ends or nicks. *J. Am. Chem. Soc.*, **133**, 3219–3221.
59. Huang,Z., Tong,Y., Wang,J. and Huang,Y. (2003) NMR studies of the relationship between the changes of membrane lipids and the cisplatin-resistance of A549/DDP cells. *Cancer Cell Int.*, **3**, 5.
60. Brennan,L.D., Forties,R.A., Patel,S.S. and Wang,M.D. (2016) DNA looping mediates nucleosome transfer. *Nat. Commun.*, **7**, 13337.
61. An,W., Kim,J. and Roeder,R.G. (2004) Ordered cooperative functions of PRMT1, p300, and CARM1 in transcriptional activation by p53. *Cell*, **117**, 735–748.
62. Knezetic,J.A. and Luse,D.S. (1986) The presence of nucleosomes on a DNA template prevents initiation by RNA polymerase II in vitro. *Cell*, **45**, 95–104.
63. Todd,R.C. and Lippard,S.J. (2010) Consequences of cisplatin binding on nucleosome structure and dynamics. *Chem, Biol.*, **17**, 1334–1343.
64. McDonald,E.S., Randon,K.R., Knight,A. and Windebank,A. (2005) Cisplatin preferentially binds to DNA in dorsal root ganglion neurons in vitro and in vivo: a potential mechanism for neurotoxicity. *Neurobiol. Dis.*, **18**, 305–313.
65. Cheng,L., Li,C., Xi,Z., Wei,K., Yuan,S., Arnesano,F., Natile,G. and Liu,Y. (2019) Cisplatin reacts with histone H1 and the adduct forms a ternary complex with DNA. *Metallomics*, **11**, 556–564.
66. Wang,X. and Guo.,Z. (2007) The role of sulfur in platinum anticancer chemotherapy. *Anti-Cancer Agents Med. Chem.*, **7**, 19–34.
67. Zimmermann,T., Zeizinger,M. and Burda,J.V. (2005) Cisplatin interaction with cysteine and methionine, a theoretical DFT study. *J. Inorg. Biochem.*, **99**, 2184–2196.
68. Teuben,J.-M., van Boom,S.S.G.E. and Reedijk,J. (1997) Intramolecular migration of co-ordinated platinum from a sulfur to N^7 in the nucleopeptide Met-d(TpG) (5′-O-methioninate-N-ylcarbonylthymidine 2′-deoxyguanosine monophosphate). *J. Chem. Soc. Dalton Trans.*, 3979–3980.
69. Chen,Y., Tokuda,J.M., Topping,T., Meisburger,S.P., Pabit,S.A., Gloss,L.M. and Pollock,L. (2017) Asymmetric unwrapping of nucleosomal DNA propagates asymmetric opening and dissociation of the histone core. *Proc. Natl. Acad. Sci. U.S.A.*, **114**, 334–339.